Piotr PERZYNA*

THE THERMODYNAMICAL THEORY OF ELASTO-VISCOPLASTICITY ACCOUNTING FOR MICROSHEAR BANDING AND INDUCED ANISOTROPY EFFECTS

SUMMARY

The main objective of the present paper is the development of thermo-elasto-viscoplastic constitutive model of a material which takes into consideration induced anisotropy effects as well as observed contribution to strain rate effects generated by microshear banding. Physical foundations and experimental motivations for both induced anisotropy and microshear banding effects have been presented. The model is developed within the thermodynamic framework of the rate type covariance constitutive structure with a finite set of the internal state variables. A set of internal state variables consists of one scalar and two tensors, namely the equivalent inelastic deformation ε^p, the second order microdamage tensor ξ with the physical interpretation that $(\xi:\xi)^{1/2} = \xi$ defines the volume fraction porosity and the residual stress tensor (the back stress) α. The equivalent inelastic deformation ε^p describes the dissipation effects generated by viscoplastic flow phenomena, the microdamage tensor ξ takes into account the anisotropic intrinsic microdamage mechanisms on internal dissipation and the back stress tensor α aims at the description of dissipation effects caused by the kinematic hardening. To describe suitably the influence of both induced anisotropy effects and the stress triaxiality observed experimentally the new kinetic equations for the microdamage tensor ξ and for the back stress tensor α are proposed. The relaxation time T_m is used as a regularization parameter. To describe the contribution to strain rate effects generated by microshear banding we propose to introduce certain scalar function which affects the relaxation time T_m in the viscoplastic flow rule. Fracture criterion based on the evolution of the anisotropic intrinsic microdamege is formulated. The fundamental features of the proposed constitutive theory have been carefully discussed. The purpose of the development of this theory is in future applications for the description of important problems in modern manufacturing processes, and particularly for meso-, micro-, and nano-mechanical issues. This description is needed for the investigation by using the numerical methods how to avoid unexpected plastic strain localization and localized fracture phenomena in new manufacturing technology.

Keywords: *thermodynamical theory of elasto-viscoplasticity, microshear banding, induced anisotropy, microdamage, fracture phenomena*

TERMODYNAMICZNA TEORIA SPRĘŻYSTO-LEPKOPLASTYCZNOŚCI UWZGLĘDNIAJĄCA EFEKTY MIKROPASM ŚCINANIA ORAZ INDUKOWANEJ ANIZOTROPII

Głównym celem obecnej pracy jest opracowanie termo-sprężysto-lepkoplastycznego modelu konstytutywnego materiału, który uwzględnia efekty indukowanej anizotropii, jak również wpływ na wrażliwość materiału, prędkość deformacji spowodowanej tworzeniem się mikropasm ścinania. Przedstawiono fizykalne podstawy oraz eksperymentalne motywacje dla efektów wywołanych przez obydwa rodzaje indukowanych anizotropii oraz przez tworzenie się mikropasm ścinania. Model materiału został opracowany w ramach termodynamicznej, kowariantnej struktury konstytutywnej typu prędkościowego ze skończonym zbiorem parametrów wewnętrznych. Przyjęto, że zbiór parametrów wewnętrznych składa się z jednej wielkości skalarnej i dwóch tensorów, mianowicie z ekwiwalentnej niesprężystej deformacji ε^p, tensora mikrouszkodzeń drugiego rzędu ξ (z fizykalną interpretacją, że $(\xi:\xi)^{1/2} = \xi$ definiuje objętościowy udział porowatości) oraz tensora naprężeń resztkowych α. Ekwiwalentna niesprężysta deformacja ε^p opisuje efekty dyssypacji generowane przez zjawisko lepkoplastycznego płynięcia, tensor mikrouszkodzeń ξ uwzględnia anizotropowe mechanizmy wewnętrznego mikrouszkodzenia w opisie wewnętrznej dyssypacji, natomiast tensor α opisuje efekty dyssypacji wywołane kinematycznym wzmocnieniem materiału. Aby opisać wpływ efektów obydwu indukowanych anizotropii i uwzględnienia efektów trójosiowości stanu naprężenia zaobserwowanych doświadczalnie zaproponowano nowe równanie kinetyczne dla tensora mikrouszkodzenia ξ i dla tensora naprężeń resztkowych α. Czas relaksacji T_m został wykorzystany jako parametr regularyzacji. Aby opisać udział wrażliwości materiału na prędkość deformacji generowanego przez tworzenie się mikropasm ścinania, zaproponowano wprowadzenie pewnej funkcji skalarnej, która wpływa na czas relaksacji T_m w procesie płynięcia lepkoplastycznego. Sformułowano kryterium zniszczenia bazujące na ewolucji anizotropowego wewnętrznego mikrouszkodzenia. Przeprowadzono szczegółową analizę wszystkich podstawowych cech zaproponowanej teorii konstytutywnej. Opracowana teoria może być wykorzystana w przyszłości do opisu ważnych problemów związanych z technologicznymi procesami, w szczególności dla zbadania zjawisk w meso-, micro-, i nanomechanice. Te opisy są potrzebne do szczegółowego zbadania za pomocą metod numerycznych jak uniknąć niepotrzebnych plastycznych lokalizacji oraz zjawiska zlokalizowanego zniszczenia w nowych procesach technologicznych.

Słowa kluczowe: *termodynamiczna teoria sprężysto-lepkoplastyczności, mikropasma ścinania, indukowana anizotropia, zjawiska zniszczenia*

* Institute of Fundamental Technological Research, Polish Academy of Sciences, Warsaw, Poland

1. PROLOGUE

Experimental observations concerning investigation of dynamic loading processes have shown that formation of microshear bands influences the evolution of microstructure of material. We can conclude that microshear banding contributes to viscoplastic strain rate effects. On the other hand analysis of recent experimental observations concerning investigations of fracture phenomena under dynamic loading processes suggests that there are two kinds of induced anisotropy:

(i) The first caused by the residual type stress produced by the heterogeneous nature of the finite plastic deformation in polycrystalline solids;

(ii) The second the fracture induced anisotropy generated by the evolution of the microdamage mechanism. It is noteworthy to stress that both these induced anisotropy effects are coupled.

In recent years there has been great activity in the field of continuum mechanics to describe anisotropic effects on fracture phenomena. This trend in research has been particularly valuable in the continuum damage mechanics, cf. Boehler (1990) and Voyiadjis, Ju and Chaboche (1998). Analysis of recent experimental results concerning investigations of fracture phenomena under dynamic loading processes suggests that there are three main reasons for anisotropic effects:

(i) The strain induced anisotropy is caused by the residual type stresses which result from the heterogeneous nature of the plastic deformation in polycrystalline materials. Experimental evidence indicates that yield surfaces exhibit anisotropic hardening. Subsequent yield surfaces are both translated and deformed in stress space. In phenomenological description this kind of anisotropy is modelled by the shift of the yield surface in stress space. This shift of the yield surface might be described by the residual stress tensor (the back stress) α introduce as the internal state variable.

(ii) The anisotropy caused by the formation of localized shear bands and the evolution of microdamage process along the localized regions.

(iii) The anisotropy induced by the evolution of the intrinsic microdamage process. Experimental observations have shown that in the microdamage process the generated anisotropy is a consequence of rather random phenomena connected with some directional property of the formation of microcracks. This anisotropic effect is very much affected by the crystallographic structure of a material as well as by small fluctuations (due to wave interactions) of the applied stress tensor at particular point of a body during dynamic process.

The main objective of the present paper is the development of thermo-elasto-viscoplastic constitutive model of a material which, takes into consideration observed contribution to strain rate effects generated by microshear banding, as well as both mentioned earlier induced anisotropy effects.

The model is developed within the thermodynamic framework of the rate type covariance constitutive structure with a finite set of the internal state variables. A set of internal state variables consists of one scalar and two tensors, namely equivalent inelastic deformation ε^p, the second order microdamage tensor ξ with the physical interpretation that $(\xi : \xi)^{1/2} = \xi$ defines the volume fraction porosity and the residual stress (the back stress) tensor α. The equivalent inelastic deformation ε^p describes the dissipation effects generated by viscoplastic flow phenomena, the microdamage tensor ξ takes into account the anisotropic intrinsic microdamage mechanisms on internal dissipation and the back stress tensor α aims at the description of dissipation effects caused by the kinematic hardening, cf. Perzyna and Voyiadjis (2005).

To describe suitably the influence of both induced anisotropy effects and the stress triaxiality the new kinetic equations for the microdamage tensor ξ and for the back stress tensor α are proposed. The relaxation time is used as a regularization parameter. To describe the contribution to strain rate effect generated by microshear banding we propose to introduce certain scalar function which affects the relaxation time T_m in the viscoplastic flow equation (cf. Nowak, Perzyna and Pecherski 2007). By assuming that the relaxation time tends to zero the thermo-elasto-plastic (rate independent) response of the damage material can be obtained. Fracture criterion based on the evolution of the anisotropic intrinsic microdamage is formulated. Very important part of this constitutive modelling is the identification procedure for the material functions and constants involved in the constitutive equations proposed. This procedure has been developed in the papers Glema, Lodygowski, Nowak, Perzyna and Voyiadjis (2005) and Glema, Lodygowski, Perzyna and Sumelka (2006).

2. PHYSICAL FOUNDATIONS

2.1. Physical origin of elastic-viscoplastic response of solids

The high-rate deformation of face-centered cubic (f.c.c.) metals, such as copper, aluminum, lead and nickel has been recently extensively studied (cf. review paper by Follansbee 1986). It has been shown that the apparent strain rate sensitivity of f.c.c. metals has two origins: that associated with the finite velocity of dislocations, and that connected with the evolution of the dislocation substructure. The first of these two components – the instantaneous rate sensitivity – is related to the wait – times associated with thermally activated dislocation motion. The second component has more to do with the relative importance of dislocation generation and annihilation at different strain rates, and shall be referred to as the strain rate history effect.

The rate and temperature dependence of the flow stress of metal crystals can be explained by different physical mechanisms of dislocation motion. The microscopic processes combine in various ways to give several groups of deformation mechanisms, each of which can be limited to the particular range of temperature and strain rate changes (cf. Perzyna 2005).

It will be profitable for further considerations to discuss the interaction of the thermally activated and phonon dumping mechanisms.

2.2. Interaction of the thermally activated and phonon damping mechanisms

If a dislocation is moving through the rows of barriers, then its velocity can be determined by the expression (cf. Fig.1)

$$v = AL^{-1} / (t_S + t_B) \tag{1}$$

where:

- AL^{-1} – average distance of dislocation movement after each thermal activation,
- t_S – time a dislocation spent at the obstacle,
- t_B – time of travelling between the barriers.

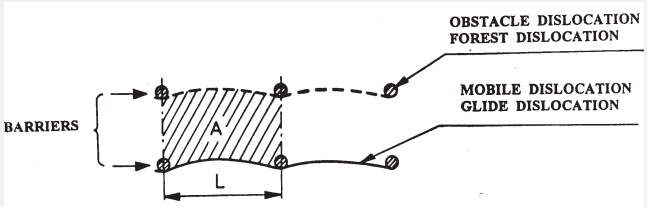

Fig. 1. Intersection of forest dislocations

The shearing rate in single slip is given by the relationship (cf. Kumar and Kumble 1969, Teodosiu and Sidoroff 1976 and Perzyna 1977, 1988, 2002, 2005)

$$\dot{\varepsilon}_p = \frac{1}{T_{mT}} \left\langle \exp\{U[(\tau - \tau_\mu)Lb]/k\vartheta\} + \right.$$
$$\left. + BAL^{-1} v / (\tau - \tau_B) b \right\rangle^{-1} \tag{2}$$

where U is the activation energy (Gibbs free energy), b denotes the Burgers vector, k is the Boltzmann constant, ϑ actual absolute temperature, B denotes the dislocation drag coefficient, v is the frequency of vibration of the dislocation, τ_μ denotes the athermal stress and τ_B is attributed to the stress needed to overcome the forest dislocation barriers to the dislocation motion and is called the back stress.

The two relaxation times

$$\frac{1}{T_{mT}} \frac{b\tau_B}{BAL^{-1}v} = \frac{\alpha b^2 \tau_B}{B} = \frac{1}{T_{mD}} \tag{3}$$

and two effective resolved shear stresses

$$\tau^*_T = \tau - \tau_\mu \quad \text{and} \quad \tau^*_D = \tau - \tau_B \tag{4}$$

are separately defined for the thermally activated and phonon damping mechanisms, respectively.

If the time t_B taken by the dislocation to travel between the barriers in a viscous phonon medium is negligible when compared with the time t_S spent at the obstacle, then

$$v = \frac{AL^{-1}}{t_S} \tag{5}$$

and we can focus our attention on the analysis of the thermally activated process.

When the ratio t_B/t_S increases then the dislocation velocity (1) can be approximated by the expression

$$v = \frac{AL^{-1}}{t_B} \tag{6}$$

for the phonon damping mechanism.

It is noteworthy to stress that the relaxation time varies when the mechanism of the dislocation motion changes from the thermally activated to the phonon damping.

3. EXPERIMENTAL MOTIVATION FOR MICROSHEAR BANDING EFFECTS

3.1. Experimental observations of single crystal behaviour

Rashid *et al*. (1992) performed an experimental study of highly heterogeneous deformations in copper single crystals to investigate the importance of the dislocation substructure. Their experimental results are mainly qualitative in nature, and include optical photographs and micrographs of the deformed specimens, and scanning and transmission electromicrographs of the substructure. The results obtained seem to support the earlier findings related to the strain rate history dependence of the substructure evolution. The higher total dislocation density observed in the notch region of the dynamically deformed specimen, as compared to the same region in the quasi-statically deformed specimen, reflects the higher shear stress attained in the dynamic case.

When ductile single crystals of metals are finitely deformed, they display highly heterogeneous deformation, e.g. when crystals are stretched in tension, they can neck and then develop macroscopic bands of localized shearing (cf. Fig. 2).

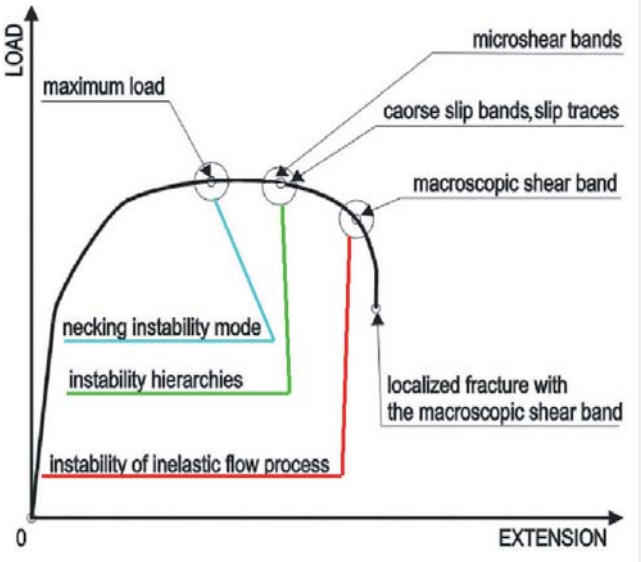

Fig. 2. One dimensional loading tests

Experimental observations of Chang and Asaro (1980, 1981), Lisiecki *et al*. (1982) and Spitzig (1981) for copper, aluminum – copper and nitrogenated Fe–Ti–Mn single crys-

tals investigated in uniaxial tension tests have shown that in the first stage of the process, a crystal specimen undergoes uniform extension in single slip. At the point when the load--engineering strain trajectory reaches its maximum, a crystal specimen exhibits slight amounts of very diffuse necking, (cf. Figs 3, 4 and 5). The neck is usually symmetric in shape indicating that double slip is operative within it, cf. Lisiecki *et al*. (1982). At this stage of the tensile process, the gross plastic deformations are localized to the diffusely necked region and the thermomechanical coupling effects begin to play a crucial role. That is why in this region of the specimen the tensile process has to be considered as adiabatic. With continued extension the macroscopic, adiabatic shear bands have soon developed within the diffusely necked region.

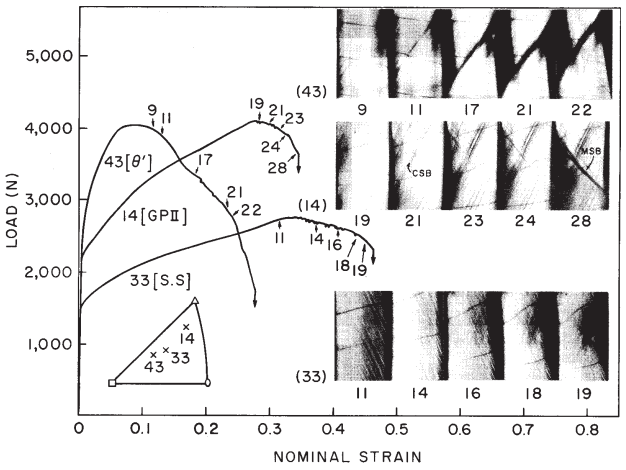

Fig. 3. Load versus engineering strain curves for various ageing treatments. Numbered photos correspond to the indicated points on the load-strain curves (after Chang and Asaro 1981)

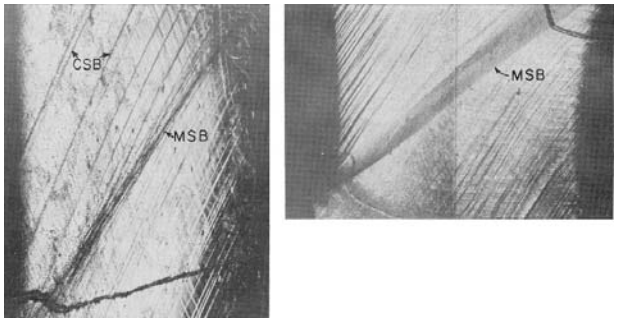

Fig. 4. Coarse slip band (CSB) and macroscopic shear bands (MSB) in (a) GPII tested at 77 K and (b) a θ′ strengthened crystal tested at 298 K (after Chang and Asaro 1981)

It has been experimentally observed that at the inception of the macroscopic, adiabatic shear band, the direction of the band is slightly different from the detected coarse slip bands or slip traces. In other words, the macroscopic shear bands are not aligned with the active slip systems in the crystal's matrix but are misaligned by angle δ, (cf. Figs 4 and 5).

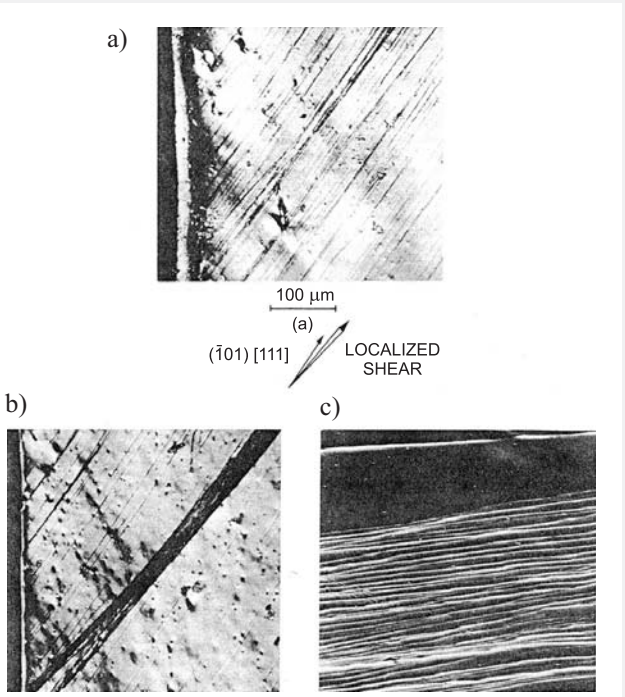

Fig. 5. Slip traces and localized shear on the surface of nitrogenated Fe–Ti–Mn crystal of orientation D deformed at 295 K: a) initial deformation until necking began; b) subsequent deformation after removal of neck and lecalized sheer bands from initial deformation; c) slip traces within localized shear band in (b) (after Spitzig 1981)

3.2. Heuristic considerations

From the analysis of the experimental investigations of localized shearing in single crystals performed by Chang and Asaro (1980, 1981), Spitzig (1981), Lisiecki *et al*. (1982) and Rashid *et al*. (1982) we can follow the events in the order in which things naturally happen within a gauge length of the specimen during the uniaxial test, (cf. Figs 2 and 6).

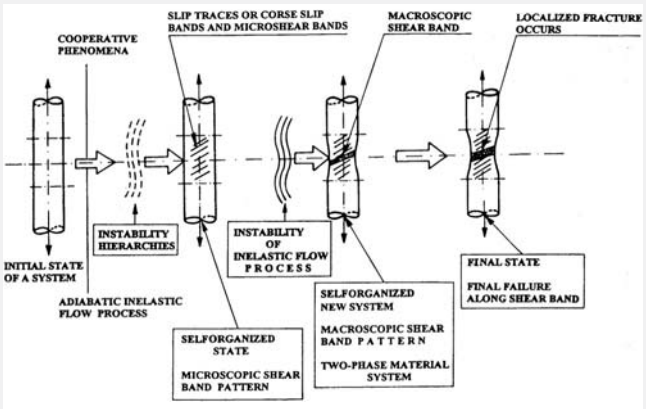

Fig. 6. Subsequent states of adiabatic inelastic flow process of single crystal

In the first stage of the adiabatic inelastic flow process a crystal specimen (a system) undergoes uniform extension and slip takes place. When control parameters are changed over a wide range, our system may run through a hierarchy of instabilities and accompanying cooperative phenomena.

When we look at a microscopic level we observe that a crystal is well ordered, and is self organized in microscopic shear band pattern.

At the point when the load-engineering strain trajectory reaches its maximum, i.e. when the criterion of the onset of the localization by necking mode is satisfied, a crystal specimen exhibits slight amount of very diffuse symmetric necking.

With continued extension the instability of inelastic flow process takes place and we observe on macroscopic level the formation of adiabatic shear band pattern within the diffusely necked region. A system is self organized to a new – two-phase material system (cf. Fig. 6). This is mainly due to different substructure and its evolution within the regions of adiabatic shear bands when compared with the substructure in the attached zones (cf. Fig. 6). Final separation occurs by a ductile failure mechanism along the shear band, (cf. Figs 2 and 6).

3.3. Viscoplastic model of single crystals

The main idea of the viscoplastic flow mechanism is to accomplish in one model the description of behaviour of single crystals valid for the entire range of strain rate changes. In other words, the main conception is to encompass the interaction of the thermally activated and phonon damping mechanisms.

To achieve this aim the empirical overstress function Φ has been introduced and the strain rate is postulated in the form as follows (cf. Perzyna 1988)

$$\dot{\varepsilon}^p = \frac{1}{T}\langle \Phi\left[\frac{\tau}{\tau_Y(\varepsilon^p, \vartheta, \beta, \zeta)} - 1\right]\rangle \operatorname{sgn}\tau \tag{7}$$

where T is the relaxation time, $\langle\cdot\rangle$ denotes the Macauley bracket and τ_Y is the static yield stress function. In this model the static yield stress function depends on the inelastic strain ε^p, temperature ϑ, the density of obstacle dislocations β and the concentration of point defects ζ.

It is noteworthy that the empirical overstress function Φ can be determined basing on available experimental results performed under dynamic loading.

3.4. Strain rate sensitivity

In previous sections fundamental features of finite deformation, rate dependent plastic flow of crystalline solids were discussed from microscopic and macroscopic phenomenological points of view. Particular viscoplastic flow model was proposed to predict deformation textures and large strain, temperature and rate dependent and strain hardening behaviour of polycrystals from the known behaviour of single crystals.

The possibility of making such a prediction rests on the tacit assumption that the mechanisms of plastic deformation in aggregates are substantially identical with those observed in single crystals.

Experimental justifications of the thermally activated and phonon damping mechanisms as well as the discussion of their range rate and temperature changes for particular materials have been given in many papers. Particular importance for our purposes have results obtained by Campbell and Ferguson (1970). In their paper an account is given of experiments in which the shear flow stress of mild steel was measured at temperature from 195 to 713 K and strain rate from 10^{-3} to $4 \cdot 10^4$ s^{-1}. The flow stress at lower yield is plotted in Figure 7 as shear stress against the logarithm of shear strain rate, for the various temperatures used throughout the investigation.

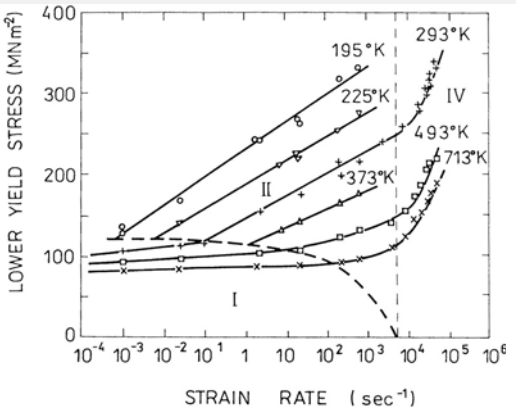

Fig. 7. Variation of lower yield stress with strain rate, at constant temperature (after Campbell and Ferguson 1970)

For the purpose of the discussion which follows, it is convenient to divide the curves into three regions, each corresponding to a certain range of strain rate which is a function of the temperature. Following Rosenfield and Hahn (1966) these will be referred to as region I, II and IV. These regions are indicated in Figure 7.

In region I the flow stress shows a small temperature and strain rate sensitivity, the latter decreasing with increasing temperature. Prestraining increases the flow stress but has little effect on the rate sensitivity of the flow stress, $(\partial\tau / \partial \ln \dot{\varepsilon}^p)_\vartheta$, at room temperature. The dominant factor in region I seems to be the long-range internal stress fields due to dislocations, precipitate particles, grain boundaries etc.

In region II the flow stress shows greater rate and temperature sensitivities. From a survey of their own and previous work, Rosenfield and Hahn (1966) concluded that in this region the rate sensitivity $(\partial\tau / \partial \ln \dot{\varepsilon}^p)_\vartheta$ is independent of temperature and strain rate. However, the data of Campbell and Ferguson (1970) show a consistent increase in $(\partial\tau / \partial \ln \dot{\varepsilon}^p)_\vartheta$ as temperature is reduced.

It has been suggested by Campbell and Ferguson (1970) that the flow behaviour throughout region II can be explained by the thermal activation of dislocation motion.

Since the relaxation time T_{mT} is related to the dislocation structure it may be governed by the deformation history, rather than a function of the state variables ε^p, τ and ϑ.

The experimental data obtained by Campbell and Ferguson (1970) for mild steel in region II are properly interpreted by the linear approximation of the thermally activated theory.

Region IV is characterized by a rapid increase in semi-logarithmic rate sensitivity $(\partial\tau/\partial\ln\dot{\varepsilon}^p)_\vartheta$ with increasing strain rate, this parameter being approximately independent of temperature in the range 293 to 713 K.

In Figure 8 the experimental data of Campbell and Ferguson (1970) for region IV are replotted using a linear strain-rate scale, and it is seen that, within the accuracy of measurement, they can be represented by straight lines at all three temperatures and all three values of pre-strain. While the slopes of these lines show only a small dependence on temperature, their intercepts on the stress axis vary greatly with temperature.

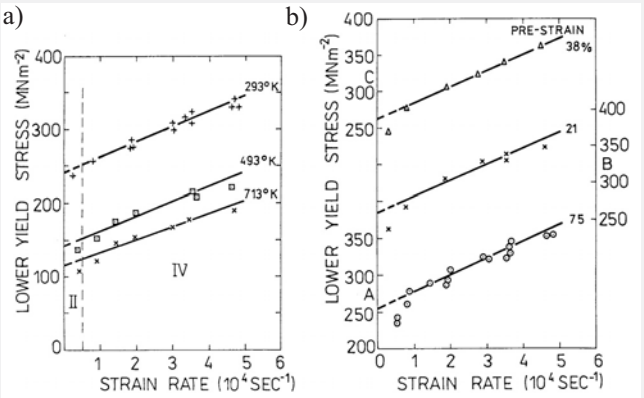

Fig. 8. Variation of lower yield stress with strain rate (region IV): a) zero pre-strain; temperature 293, 493, 713 K; b) pre-strain 7.5, 21, 38%; temperature 293 K. After Campbell and Ferguson (1970)

According to the interpretation presented by Campbell and Ferguson (1970), the intercepts in Figure 8 are determined by the temperature-dependent barrier stress $\tau_\mu + U_o/\upsilon^*$ (U_o denotes the activation energy for intersection at zero effective stress and υ^* the activation volume), at which the strain rate reaches $1/T_{mT}$. When the applied stress exceeds this barrier stress, the time required to activate a dislocation past the short-range barriers of obstacles is negligible, hence its velocity is controlled by dissipation of energy as it moves through the lattice. Assuming that this dissipation is of a linear viscous nature, the excess stress τ_D will be proportional to the strain rate $\dot{\varepsilon}^p$, i.e.

$$\tau_D = \eta\dot{\varepsilon}^p, \tag{8}$$

where η denotes the macroscopic viscosity. Equating τ_D to the difference between the applied stress and the barrier stress $\tau_B = \tau_\mu + U_o/\upsilon^*$, we obtain for region IV

$$\tau = \tau_B + \eta\dot{\varepsilon}^p. \tag{9}$$

Comparison (9) with $(3)_2$ under the condition that $\tau = \tau_B(1 + T_{mD}\dot{\varepsilon}^p)$ gives

$$\eta = T_{mD}\tau_B = \frac{B}{\alpha b^2}. \tag{10}$$

The values of η can be obtained from the slops of the lines of Figure 8.

For room temperature and zero pre-strain we have the relaxation time as follows

$$T_{mD} = \frac{\eta}{\tau_B} = \frac{2.1\cdot 10^3}{250\cdot 10^6}\ \text{s} = 0.84\cdot 10^{-5}\ \text{s}.$$

For 493 K and zero pre-strain

$$T_{mD} = \frac{2.0\cdot 10^3}{150\cdot 10^6}\ \text{s} = 1.3\cdot 10^{-5}\ \text{s}.$$

For 713 K and zero pre-strain

$$T_{mD} = \frac{1.8\cdot 10^3}{120\cdot 10^6}\ \text{s} = 1.5\cdot 10^{-5}\ \text{s}.$$

Thus, in the phonon viscosity damping region IV the relaxation time is a function of temperature and is not sensitive to pre-stressing (for room temperature).

For region II the relaxation time T_{mT} is obtained as constant value

$$T_{mT} = 2\cdot 10^{-4}\ \text{s},$$

while in region IV the relaxation time T_{mD} is temperature dependent and can change from $T_{mD} = 0.8\cdot 10^{-5}$ s to $T_{mD} = 1.5\cdot 10^{-5}$ s.

For the viscoplastic model of polycrystalline solids the relaxation time T_m governs the viscoplastic flow in the entire range of strain rate changes and for classical models it is generally assumed as constant value. However, in real case it has to be a function of the rate of inelastic deformation $\dot{\varepsilon}^p$, and can be determined based on experimental data (cf. Fig. 9).

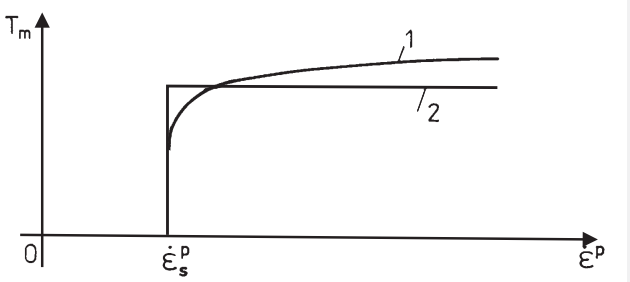

Fig. 9. Variation of the relaxation time with strain rate for mild steel (1) real case; (2) assumption for classical elasto-viscoplasticity

Another possible idea has been presented by Perzyna (1980), namely that

$$T_m = \frac{\phi}{\gamma}, \tag{11}$$

where ϕ is the control function and γ is the temperature dependent viscosity coefficient. The dimensionless control function $\phi$is assumed to depend on strain rate. Thus we have

$$T_m = \frac{1}{\gamma(\vartheta)}\phi\left(\frac{\dot{\varepsilon}^p}{\dot{\varepsilon}^p_s} - 1\right). \tag{12}$$

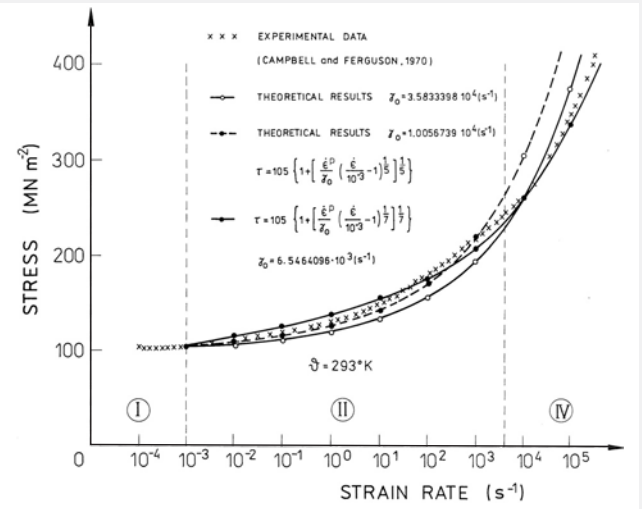

Fig. 10. Comparison of theoretical description with experimental results

In Figure 10 the theoretical results obtained by Perzyna (1980) are compared with experimental data of Campbell and Ferguson (1970) for room temperature (293 K). Taking the best fitting curve we have

$$T_m = \frac{1}{6.55\cdot 10^3}\left(\frac{\dot{\varepsilon}^p}{10^{-3}} - 1\right)^{\frac{1}{7}} (\mathrm{s}). \tag{13}$$

Figure 11 shows the plots of the relaxation time (13) and (12) for $\phi = \aleph(\cdot)$, i.e. for ϕ assumed as the Heaviside function.

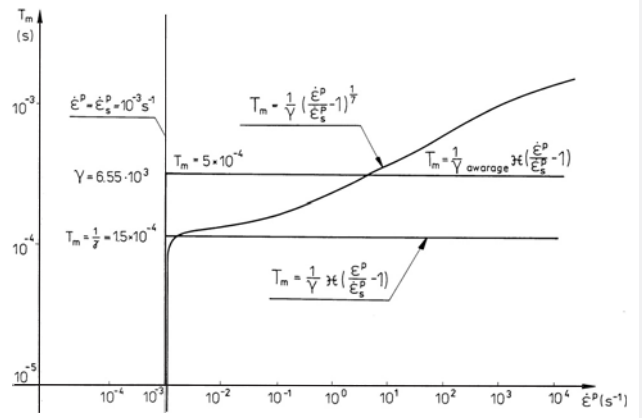

Fig. 11. Variation of the relaxation time with strain rate for variuos assumption

Dowling, Harding and Campbell (1970) investigated the strain-rate sensitivity of the yield and flow stress of aluminum, copper, brass and mild steel over a range of strain rates from 10^{-3} to $4 \cdot 10^4$ s^{-1}. These experimental data can also be used for determination of the overstress function Φ and the relaxation time T_m for these metals.

Basing on the analysis of experimental observations for single crystals and polycrystalline metals we can conclude that microshear banding influences very much a substructure of a material under consideration. As a result of this it contributes to viscoplastic strain rate effects. We have also shown that the relaxation time T_m depends on the active microshear band fraction f_{ms} and on the rate of equivalent viscoplastic deformation $\dot{\varepsilon}^p$.

4. EXPERIMENTAL MOTIVATION FOR INDUCED ANISOTROPY EFFECTS

For our considerations of anisotropic effects, the metallurgical aspects of fracture and spalling have great importance. Effects of parameters such as grain size and substructure, crack/void initiation sites, micromechanical aspects of growth, and coalescence can influence fracture and spalling mechanisms. To show the complexity of the anisotropy phenomena in microdamage process we shell discuss several available experimental results.

The most popular dynamical experiment[1)] in the investigation of the fracture phenomenon in metals is a plate-impact configuration system. This experimental system consists of two plates, a projectile plane plate impacts against a target plane. This is a good example of a dynamic deformation process. If impact velocity is sufficiently high the propagation of a plastic wave through the target is generated. The reflection and interaction of waves result a net tensile pulse in the target plate. If this stress pulse has sufficient amplitude and sufficient time duration, it will cause separation of the material and spalling process.

The reason for choosing this particular kind of dynamical experiment is that postshot photomicrographic observations of the residual porosity are available, and the stress amplitude and pulse duration can be performed sufficiently great to produce substantial porosity and the spall of the target plate.

The experimental data presented by Seaman, Curran and Shockey (1976) illustrate damage phenomena and provide a common basis for considering damage criteria. They have used a plate-impact configuration system. Following the compression waves resulting from the impact, rarefaction waves have intersected near the middle of the target plate to cause damage in the form of nearly spherical voids. The heaviest damage is localized in a narrow zone, which is called the spall plane. Both the number and the size of voids decrease with distance from this zone. This type of damage is termed ductile fracture because of high ductility (ability to flow) required of the plate material (Fig. 12).

The final damage of the target plate (aluminium 1145) for a constant shot geometry but for different impact velocities has been performed by Barbee, Seaman, Crewdson and Curran (1972). The results suggest dependence of spalling process on the pulse amplitude (Fig. 13).

[1)] For a thorough discussion of the experimental and theoretical works in the field of dynamic fracture and spalling of metals please consult the review papers by Meyers and Aimone (1983) and Curran, Seaman and Shockey (1987), cf. also Meyers (1994).

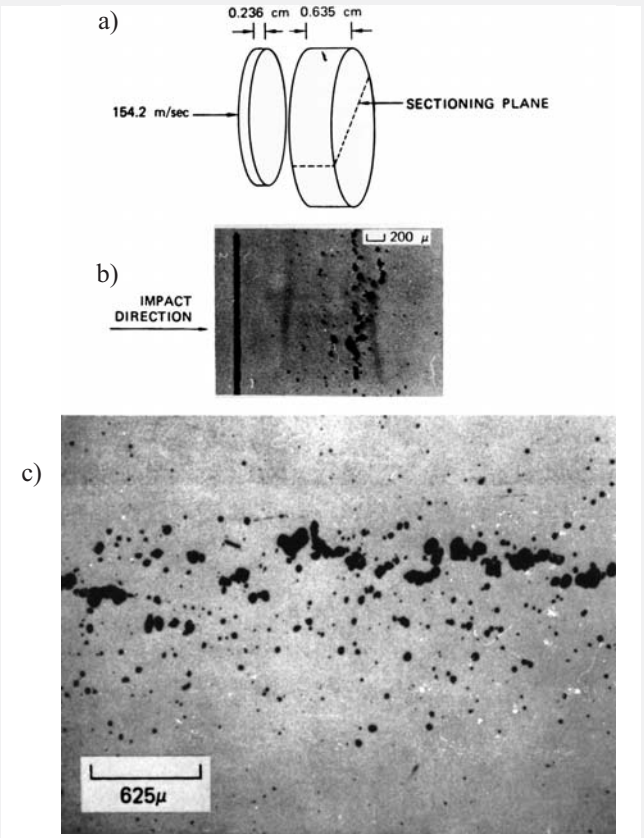

Fig. 12. A cross section of an aluminum target plate that has undergone a planar impact by another aluminum plate: a) impact configuration system; b) observed ductile fracture on a cross section through target; c) magnification of (b) (after Seaman, Curran and Shockey 1976)

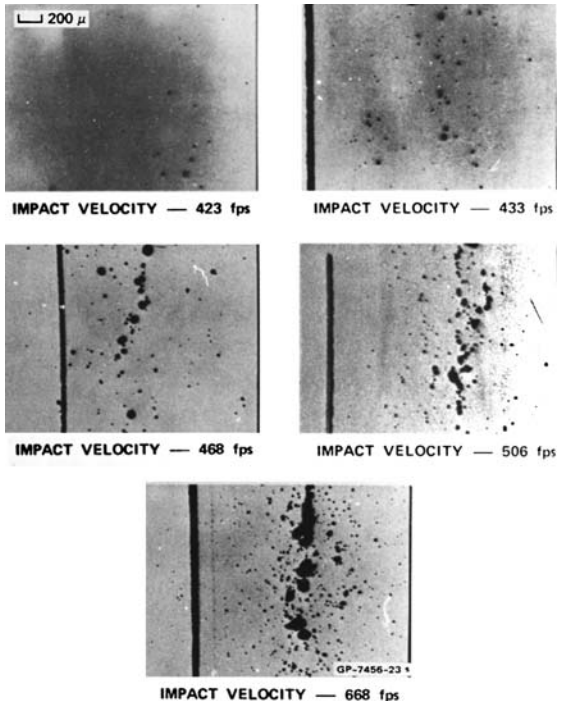

Fig. 13. The final damage of the aluminum 1145 target plate for a constant shot geometry but for different impact velocities (after Barbee, Seaman, Crewdson and Curran 1972)

A sample of full separation is shown in Figure 14, an aluminium target impacted by a plate has been damaged to the extent that full separation occurred near the center of the target, cf. Seaman, Curran and Shockey (1976). The authors suggested that this full separation appears as a macrocrack propagating through heavily damaged material. The macrocrack occurs as a result of coalescence of microvoids which is also visible in Figure 14.

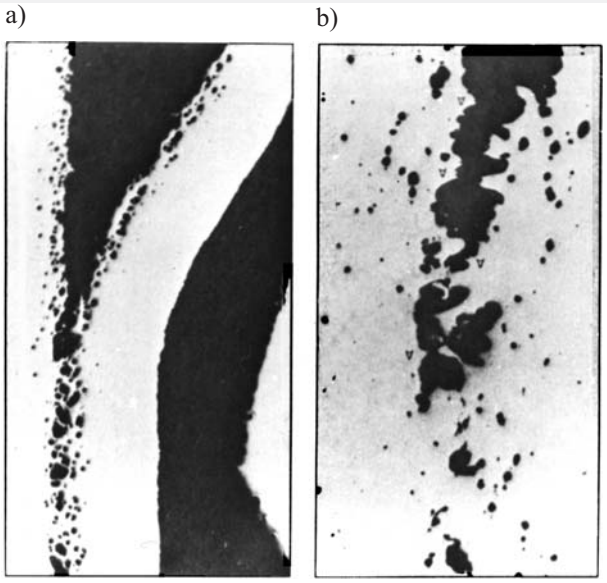

Fig. 14. A sample of full separation of an aluminum target: a) ductile crack propagation by void coalescence; b) tip of ductile crack shown in (a), at higher magnification. Impact test performed by Seaman, Curran and Shockey (1976)

Spalling by ductile void formation in nickel is characterized by ellipsoidal cracks with large axes perpendicular to the direction of the applied tensile stress (cf. Fig. 15). A more advanced microdamage process has been shown in Figure 16, where crack nucleation growth, and coalescence mechanisms in nickel have been observed.

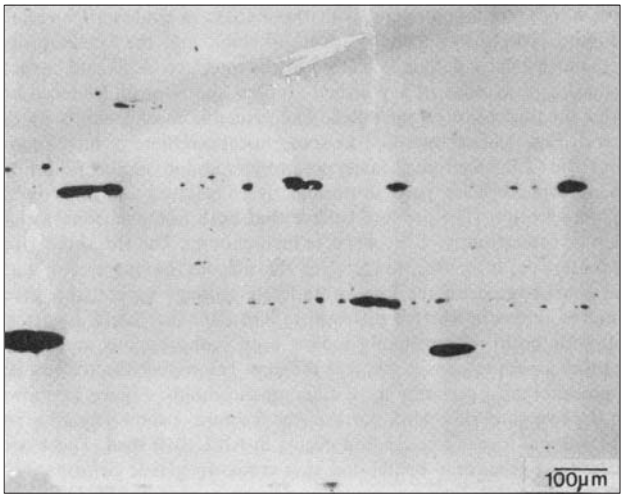

Fig. 15. Spalling by ductile void formation in nickel (after Shockey, Seaman and Curran 1973)

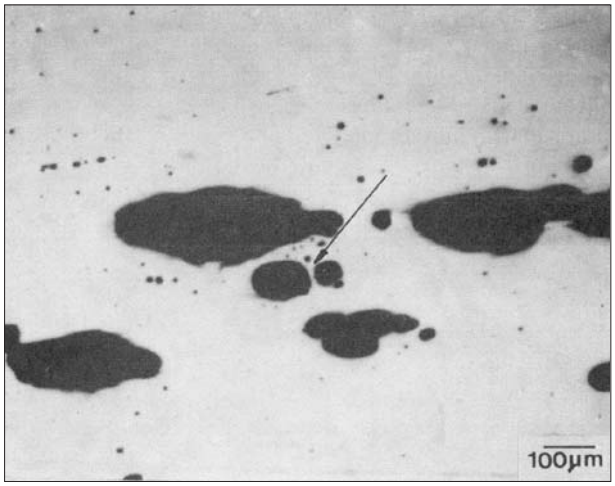

Fig. 16. Void nucleation, growth, and coalescence observed in nickel (after Shockey, Seaman and Curran 1973)

An example of brittle fracture for Armco iron is presented in Figure 17 (cf. Curran, Seaman and Shockey 1981). It shows the polished cross section through plate impact specimen with very well visible cleavage (penny shape) microcracks. The damage, which appears as randomly oriented planar microcracks, depends on the impact velocity as well as on the duration of the tensile wave. The second property is directly observed from the results presented in Figure 18 (cf. Curran, Seaman and Shockey 1977). Use of a tapered flyer results in longer tensile impulses at the thicker end. As it is shown in Figure 18 these longer pulses lead to greater damage in the Armco iron target (the inset gives to approximate durations of the tensile pulses). The damage observed in this experiment is termed brittle, although the microcrack growth is much slower than elastic crack velocities, indicating considerable plastic flow at micro crack tips.

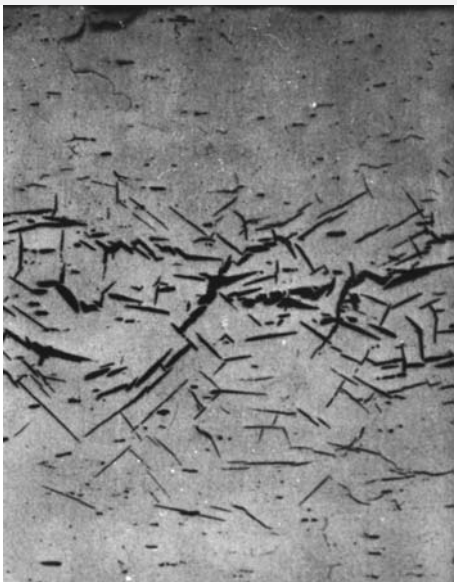

Fig. 17. Internal cleavage (penny shape) microcracks caused by shock loading in the polished cross section of an Armco iron specimen (after Curran, Seaman and Shockey 1981)

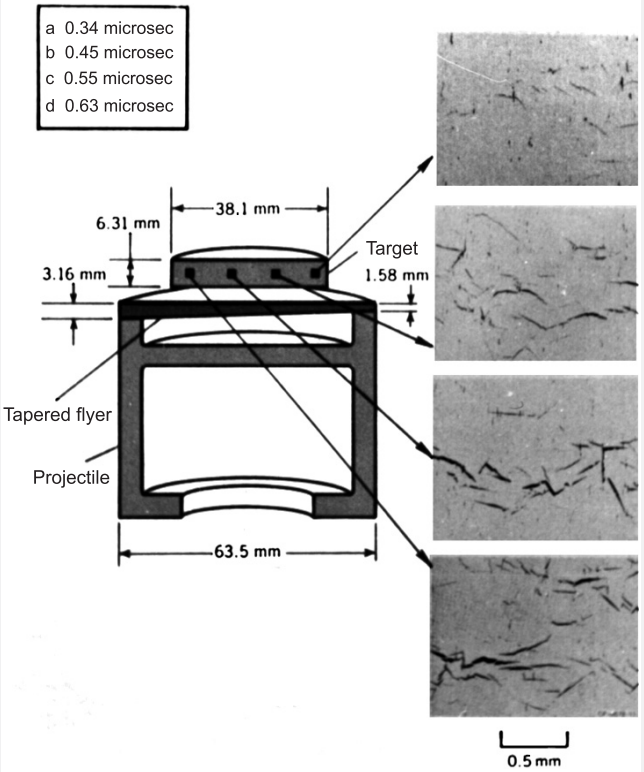

Fig. 18. Tapered flyer impact experimental results for the Armco iron target (after Curran, Seaman and Shockey 1977)

Adiabatic shear band localization during dynamic process can be another good example of anisotropic effects. Shear band form in one direction, which is determined by the state of stress and the properties of the material of a body, as well as by the boundary conditions.

Grebe, Pak and Meyers (1985) were conducted ballistic impact experiments on 12.5 mm thick commercial purity titanium and T–6pct Al–4pct V alloy plates using steel projectiles with 10.5 mm diameter. The impact velocities in their experiments varied between 578 m/s and 846 m/s. The microstructural damage mechanisms associated with shear band formation, shock wave and dynamic fracture were investigated by optical and scanning and transmission electron microscopy. The shear band were found along the two sides of the cross-section passing through the axis of the projectile. The measured shear band width in T6A14V varied between 1 and 10 μm.

Observations of the onset of fracture along the shear band were also conducted. Spherical and ellipsoidal microcracks in T6A14V were found along the bands (Fig. 19). The mechanism of final failure in T6A14V is a simple propagation of a macrocrack along the damaged material within the shear band region. In the explanation of the phenomenon of fracture along shear band very important role has the microdamage process which consists of the nucleation, growth and coalescence of microvoids.

The investigations reported by Grebe, Pak and Meyers (1985) indicated that in dynamic processes the shear band regions behave differently than adjacent zones (cf. Fig. 19).

Within the shear band region the deformation process is characterized by very large strains (shear strains over 100%) and very high strain rates (10^3–10^5 s^{-1}). The strain rate sensitivity of a material becomes very important feature of the shear band region and the micro-damage process is intensified.

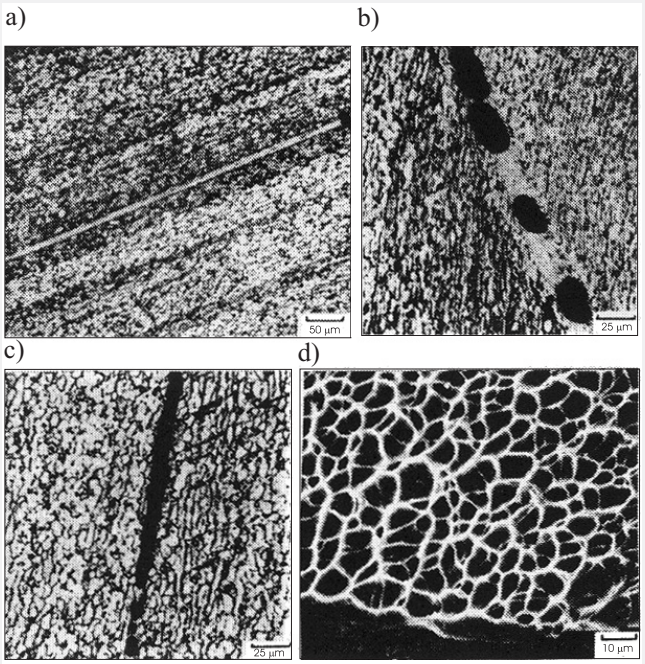

Fig. 19. Shear band in Ti6Al4V target impacted at 846 m/s (after Grebe, Pak and Meyers 1985): a) single shear band; b) microcracks in the shear band region; c) elongated macrocracks along the shear band; d) characteristic dimples observed in spall region

5. KINEMATICS OF FINITE DEFORMATION AND FUNDAMENTAL DEFINITIONS

Let $\{X^A\}$ and $\{x^a\}$ denote coordinate systems on B and S respectively. Then we refer to $B \subset \mathbf{R}^3$ as the reference configuration of a continuum body with particles $\mathbf{X} \in B$ and to $S = \phi(B)$ as the current configuration with points $\mathbf{x} \in \mathbf{S}$. The matrix $\mathbf{F}(\mathbf{X}, t) = \partial\phi(\mathbf{X}, t)/\partial\mathbf{X}$ with respect to the coordinate bases $\mathbf{E}_A(\mathbf{X})$ and $\mathbf{e}_a(\mathbf{x})$ is given by

$$F_A^a(X,t) = \frac{\partial \phi^a}{\partial X^A}(X,t) \tag{14}$$

where a mapping $\mathbf{x} = \phi(\mathbf{X}, t)$ represents a motion of a body B. We consider the local multiplicative decomposition

$$\mathbf{F} = \mathbf{F}^e \cdot \mathbf{F}^p \tag{15}$$

where $(\mathbf{F}^e)^{-1}$ is the deformation gradient that releases elastically the stress on the neighbourhood ($\phi(N(\mathbf{X}))$ in the current configuration (Fig. 20).

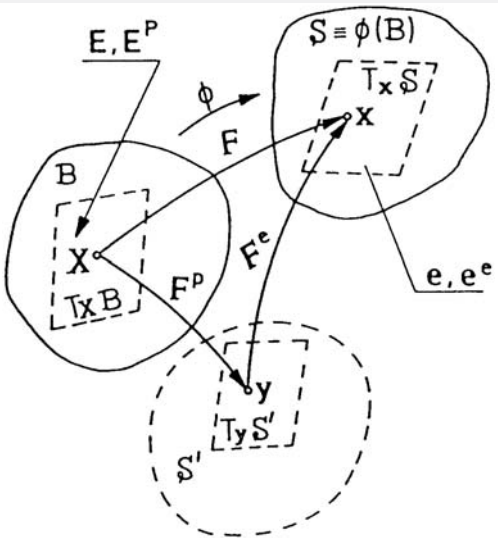

Fig. 20. Schematic representation of the multiplicative decomposition of the deformation gradient

Let us define the total and elastic Finger deformation tensors

$$\mathbf{b} = \mathbf{F} \cdot \mathbf{F}^T, \quad \mathbf{b}^e = \mathbf{F}^e \cdot \mathbf{F}^{eT} \tag{16}$$

respectively, and the Eulerian strain tensors as follows

$$\mathbf{e} = \frac{1}{2}(\mathbf{g} - \mathbf{b}^{-1}), \qquad \mathbf{e}^e = \frac{1}{2}(\mathbf{g} - \mathbf{b}^{e^{-1}}) \tag{17}$$

where $\mathbf{g}$ denotes the metric tensor in the current configuration.

By definition[2)]

$$\mathbf{e}^p = \mathbf{e} - \mathbf{e}^e = \frac{1}{2}(\mathbf{b}^{e^{-1}} - \mathbf{b}^{-1}) \tag{18}$$

we introduce the plastic Eulerian strain tensor.

To define objective rates for vectors and tensors we use the Lie derivative.[3)] Let us define the Lie derivative of a spatial tensor field $\mathbf{t}$ with respect to the velocity field υ as

$$L_\upsilon \boldsymbol{t} = \phi_* \frac{\partial}{\partial t}(\phi^* \mathbf{t}) \tag{19}$$

where ϕ^* and ϕ_* denote the pull-back and push-forward operations, respectively. The rate of deformation is defined as follows

$$\begin{aligned} \mathbf{d}^\flat &= L_\upsilon \mathbf{e}^\flat = \frac{1}{2} L_\upsilon \mathbf{g} = \\ &= \frac{1}{2}(g_{ac}\upsilon^c\big|_b + g_{cb}\upsilon^c\big|_a) e^a \otimes e^b \end{aligned} \tag{20}$$

where the symbol $\flat$ denotes the index lowering operator and $\otimes$ the tensor product,

$$\upsilon^a\big|_b = \frac{\partial \upsilon^a}{\partial x^b} + \gamma^a_{bc}\upsilon^c \tag{21}$$

[2)] For precise definition of the finite elasto-plastic deformation see Perzyna (1995).

[3)] The algebraic and dynamic interpretations of the Lie derivative have been presented by Abraham *et al*. (1988), Abraham and Marsden (1978), cf. also Marsden and Hughes (1983).

and γ^a_{bc} denotes the Christoffel symbol for the general coordinate systems $\{x^a\}$. The components of the spin ω are given by

$$\omega_{ab} = \frac{1}{2}(g_{ac}\upsilon^c\Big|_b - g_{cb}\upsilon^c\Big|_a) = \frac{1}{2}\left(\frac{\partial \upsilon_a}{\partial x^b} - \frac{\partial \upsilon_b}{\partial x^a}\right) \quad (22)$$

Similarly

$$\mathbf{d}^{e^b} = \mathrm{L}_\upsilon \mathbf{e}^{e^b}, \quad \mathbf{d}^{p^b} = L_\upsilon \mathbf{e}^{p^b} \quad (23)$$

and

$$\mathbf{d} = \mathbf{d}^e + \mathbf{d}^p \quad (24)$$

Let τ denote the Kirchhoff stress tensor related to the Cauchy stress tensor σ by

$$\tau = J\sigma = \frac{\rho_{Ref}}{\rho}\sigma \quad (25)$$

where the Jacobian J is the determinant of the linear transformation

$$\mathbf{F}(\mathbf{X},t) = (\partial / \partial X)\phi(\mathbf{X},t),$$

$\rho_{Ref}(\mathbf{X})$ and $\rho(\mathbf{x},t)$ denote the mass density in the reference and current configuration, respectively. The Lie derivative of the Kirchhoff stress tensor $\tau \in \mathbf{T}^2(S)$ (elements of $\mathbf{T}^2(S)$ are called tensors on S, contravariant of order 2) gives

$$\begin{aligned} L_\upsilon \tau &= \phi_* \frac{\partial}{\partial t}(\phi^* \tau) = \\ &= \left\{ \mathbf{F} \cdot \frac{\partial}{\partial t}[\mathbf{F}^{-1} \cdot (\tau \circ \phi) \cdot \mathbf{F}^{-1^T}] \cdot \mathbf{F}^T \right\} \circ \phi^{-1} = \\ &= \dot{\tau} - (\mathbf{d} + \omega) \cdot \tau - \tau \cdot (\mathbf{d} + \omega)^T \end{aligned} \quad (26)$$

where $\circ$ denotes the composition of mappings.

6. THERMO-ELASTO-VISCOPLATICITY CONSTITUTIVE MODEL

6.1. Constitutive postulates

Let us assume that:
(i) conservation of mass,
(ii) balance of momentum,
(iii) balance of moment of momentum,
(iv) balance of energy,
(v) entropy production inequality hold.

We introduce the four fundamental postulates:

(i) Existence of the free energy function. It is assumed that the free energy function is given by

$$\psi = \hat{\psi}(\mathbf{e}, \mathbf{F}, \vartheta; \mu) \quad (27)$$

where ϑ is temperature and μ denotes a set of the internal state variables. To extend the domain of the description of the material properties and particularly to take into consideration different dissipation effects we have to introduce the internal state variables represented by the vector μ.

(ii) Axiom of objectivity (spatial covariance). The constitutive structure should be invariant with respect to any diffeomorphism (any motion) $\zeta: S \to S$.

(iii) The axiom of the entropy production. For any regular motion of a body B the constitutive functions are assumed to satisfy the reduced dissipation inequality

$$\frac{1}{\rho_{Ref}}\tau : \mathbf{d} - (\eta\dot{\vartheta} + \dot{\psi}) - \frac{1}{\rho\vartheta}\mathbf{q} \cdot \mathrm{grad}\vartheta \geq 0 \quad (28)$$

where η is the specific (per unit mass) entropy, and $\mathbf{q}$ denotes the heat flow vector field.

(iv) The evolution equation for the internal state variable vector μ is assumed in the form as follows

$$L_\upsilon \mu = \hat{\mathbf{m}}(\mathbf{e}, \mathbf{F}, \vartheta, \mu) \quad (29)$$

where the evolution function $\hat{\mathbf{m}}$ has to be determined based on careful physical interpretation of a set of the internal state variables and analysis of available experimental observations. The determination of the evolution function $\hat{\mathbf{m}}$ (in practice a finite set of the evolution functions) appears to be the main problem of the modern constitutive modelling.

6.2. Fundamental assumptions

For our practical purposes it is sufficient to assume that the internal state vector μ has the form

$$\mu = (\varepsilon^p, \xi, \alpha) \quad (30)$$

where ε^p is the equivalent viscoplastic deformation, i.e.

$$\varepsilon^p = \int_0^t \left(\frac{2}{3}\mathbf{d}^p : \mathbf{d}^p\right)^{\frac{1}{2}} dt \quad (31)$$

ξ denote the microdamage second order tensor, with the physical interpretation that $(\xi : \xi)^{\frac{1}{2}} = \xi$ defines the volume fraction porosity and takes account for microdamaged effects and α denotes the residual stress (the back stress) and aims at the description of the kinematic hardening effects.

Let us introduce the plastic potential function

$$f = f(\tilde{J}_1, \tilde{J}_2, \vartheta, \mu),$$

where $\tilde{J}_1, \tilde{J}_2$ denote the first two invariants of the stress tensor $\tilde{\tau} = \tau - \alpha$.

Let us postulate the evolution equations as follows

$$\mathbf{d}^p = \Lambda\mathbf{P}, \quad \omega^p = \Lambda\Omega, \quad L_\upsilon \xi = \Xi, \quad L_\upsilon \alpha = \mathbf{A} \quad (32)$$

where for elasto-viscoplastic model of a material we assume (cf. Perzyna 1963, 1966, 1971, 1995, 2005)

$$\Lambda = \frac{1}{T_m}\langle \Phi\left(\frac{f}{\kappa} - 1\right)\rangle \quad (33)$$

T_m denotes the relaxation time for mechanical disturbances, the isotropic work-hardening-softening function κ is

$$\kappa = \hat{\kappa}(\varepsilon^p, \vartheta, \xi) \quad (34)$$

Φ is the empirical overstress function, the bracket $\langle\cdot\rangle$ defines the ramp function,

$$\mathbf{P}=\left.\frac{\partial f}{\partial \tau}\right|_{\xi=const}\left(\left\|\frac{\partial f}{\partial \tau}\right\|\right)^{-1} \tag{35}$$

Ω, Ξ and **A** denote the evolution functions which have to be determined.

6.3. Microshear banding effects

To decsribe the microshear banding effects let us assume that the relaxation time T_m depends on the active microshear bands fraction f_{ms} and on the rate of equivalnet viscoplastic deformation $\dot{\varepsilon}^p$ (cf. Pęcherski (1988) and Nowak, Perzyna and Pęcherski (2007)), i.e.

$$T_m = T_m(f_{ms}, \dot{\varepsilon}^P) \tag{36}$$

Additionaly we introduce the simplification as follows

$$T_m = T_m^0 \phi_1(f_{ms}) \phi_2(\dot{\varepsilon}^P) \tag{37}$$

For example, for mild steel (cf. considerations in Section 3.3) we can postulate

$$\begin{aligned}\phi_1(f_{ms}) &= [1 - f_{ms}(\varepsilon^P)] = \\ &= \left[1 - f_{ms}^0 \frac{1}{1+\exp(a - b\,\varepsilon^P)}\right]\end{aligned} \tag{38}$$

and

$$\phi_2(\varepsilon^P) = \left(\frac{\dot{\varepsilon}^P}{\dot{\varepsilon}_s^P} - 1\right)^{\frac{1}{7}} \tag{39}$$

where f_{ms}^0, a and b are material parameters. Finally we have

$$T_m = T_m^0 \left[1 - f_{ms}^0 \frac{1}{1+\exp(a - b\,\varepsilon^P)}\right]\left(\frac{\dot{\varepsilon}^P}{\dot{\varepsilon}_s^P} - 1\right)^{\frac{1}{7}} \tag{40}$$

6.4. Constitutive assumption for the plastic spin

Let us postulate that Ω has the form[4] (cf. Dafalias 1983 and Loret 1983)

$$\Omega = \eta^* (\alpha \cdot \mathbf{P} - \mathbf{P} \cdot \alpha) \tag{41}$$

where η^* denotes the scalar valued function of the invariants of the tensors α, ξ and **P**, and may depend on temperature ϑ.

To take into consideration the observed time dependent effects it is advantageous to use the proposition of the description of the intrinsic microdamage process presented by Perzyna (1986), Duszek-Perzyna and Perzyna (1994), and Dornowski and Perzyna (2000).

6.5. Anisotropic intrinsic microdamage mechanisms

Let us assume that the intrinsic microdamage process consists of the nucleation and growth mechanisms.[5]

Based on the heuristic suggestions and taking into account the influence of the stress triaxiality and anisotropic effects on the nucleation and growth mechanisms we assume the evolution equation for the microdamage tensor ξ as follows

$$\begin{aligned}L_\upsilon \xi = &\frac{\partial h^*}{\partial \tau}\frac{1}{T_m}\left\langle \Phi\left[\left[\frac{\tilde{I}_n}{\tau_n(\xi,\alpha,\vartheta,\varepsilon^p)} - 1\right]\right]\right\rangle + \\ &+ \frac{\partial g^*}{\partial \tau}\frac{1}{T_m}\left\langle \Phi\left[\left[\frac{\tilde{I}_g}{\tau_{eq}(\xi,\alpha,\vartheta,\varepsilon^p)} - 1\right]\right]\right\rangle\end{aligned} \tag{42}$$

The tensorial function $\frac{\partial h^*}{\partial \tau}$ describes the mutual microcrack interaction for nucleation mechanism, while the tensional function $\frac{\partial g^*}{\partial \tau}$ represents the mutual microcrack interaction for growth process, τ_n and τ_{eq} denote the threshold stresses for microcrack nucleation and growth, respectively.

$$\tilde{I}_n = a_1 \tilde{J}_1 + a_2 \sqrt{\tilde{J}_2'} + a_3 (\tilde{J}_3')^{\frac{1}{3}} \tag{43}$$

defines the stress intensity invariant for nucleation, a_i (i = 1, 2, 3) are the material constants, $\tilde{J}_2'$ and $\tilde{J}_3'$ are the second and third invariants of the stress deviator $\tilde{\tau}' = (\tau - \alpha)'$,

$$\tilde{I}_g = b_1 \tilde{J}_1 + b_2 \sqrt{\tilde{J}_2'} + b_3 (\tilde{J}_3')^{\frac{1}{3}} \tag{44}$$

defines the stress intensity invariant for growth and b_i (i = 1, 2, 3) are the material constants. This determines the evolution function Ξ.

In the evolution equation(42) the functions

$$h = \hat{h}(\tau, \vartheta, \varepsilon^P, \xi, \alpha) \tag{45}$$

$$g = \hat{g}(\tau, \vartheta, \varepsilon^P, \xi, \alpha) \tag{46}$$

play the fundamental role, and have to be determined based on available experimental observation data. We also introduced the denotations as follows

$$\frac{\partial h^*}{\partial \tau} = \frac{\partial \hat{h}}{\partial \tau}\left(\left\|\frac{\partial \hat{h}}{\partial \tau}\right\|\right)^{-1}, \quad \frac{\partial g^*}{\partial \tau} = \frac{\partial \hat{g}}{\partial \tau}\left(\left\|\frac{\partial \hat{g}}{\partial \tau}\right\|\right)^{-1} \tag{47}$$

The treshold stress τ_n and τ_{eq} for microcarck nucleation and growth, respectively, can be assumed as the material functions in the form

$$\tau_n = \tau_n(\xi, \alpha, \vartheta, \varepsilon^P), \quad \tau_{eq} = \tau_{eq}(\xi, \alpha, \vartheta, \varepsilon^P) \tag{48}$$

[4] For a thorough discussion of a concept of the plastic spin and its constitutive description in phenomenological theories for macroscopic large plastic deformations please consult the critical review paper by Van der Giessen (1991).

[5] Recent experimental observation results (cf. Shockey, Seaman and Curran 1985) have shown that coalescence mechanism can be treated as nucleation and growth process on a smaller scale.

6.6. Kinematic hardening

To determine the evolution function **A** we shall follow some results obtained by Duszek and Perzyna (1991). The kinematic hardening evolution law takes the form

$$L_{\upsilon}\alpha=\frac{1}{T_m}\langle\Phi(\frac{f}{\kappa}-1)\rangle\left[r_1\mathbf{P}+r_2\,\frac{\mathbf{P}:\mathbf{Q}}{\tilde{\tau}:\mathbf{Q}+r_3\xi:\mathbf{Q}}(\tilde{\tau}+r_3\xi)\right] \quad (49)$$

where r_1, r_2 and r_3 are the material coefficients and

$$\mathbf{Q}=\left[\frac{\partial f}{\partial\tau}+\left(\frac{\partial f}{\partial\xi}-\frac{\partial\kappa}{\partial\xi}\right):\frac{\partial\xi}{\partial\tau}\right]\left\|\frac{\partial f}{\partial\tau}+\left(\frac{\partial f}{\partial\xi}-\frac{\partial\kappa}{\partial\xi}\right):\frac{\partial\xi}{\partial\tau}\right\|^{-1} \quad (50)$$

The kinetic law (49) represents the linear combination of the Prager and Ziegler kinematic hardening rules and additionally depends linearly on the microdamage tensor ξ.

6.7. Thermodynamic restrictions and rate type constitutive relations

Suppose the axiom of the entropy production holds. Then the constitutive assumption (27) and the evolution equations (32) lead to the results as follows

$$\begin{aligned}&\tau=\rho_{Ref}\,\frac{\partial\hat{\psi}}{\partial\mathbf{e}},\quad \eta=-\frac{\partial\hat{\psi}}{\partial\vartheta},\\&-\frac{\partial\hat{\psi}}{\partial\mu}\cdot L_{\upsilon}\mu-\frac{1}{\rho\vartheta}\mathbf{q}\cdot\mathrm{grad}\vartheta\geq 0\end{aligned} \quad (51)$$

The rate of internal dissipation is determined by

$$\begin{aligned}\vartheta\hat{i}&=-\frac{\partial\hat{\psi}}{\partial\mu}\cdot L_{\upsilon}\mu=\\&=-\left[\frac{\partial\hat{\psi}}{\partial\varepsilon^P}\sqrt{\frac{2}{3}}+\frac{\partial\hat{\psi}}{\partial\alpha}:\left(r_1\mathbf{P}+r_2\,\frac{\mathbf{P}:\mathbf{Q}}{\tilde{r}:\mathbf{Q}+r_3\xi:\boldsymbol{Q}}\tilde{\tau}+\right.\right.\\&\left.\left.+r_3\xi\right)\right]\Lambda-\frac{\partial\hat{\psi}}{\partial\xi}:\Xi\end{aligned} \quad (52)$$

Operating on the stress relation $(51)_1$ with the Lie derivative and keeping the internal state vector constant, we obtain

$$\begin{aligned}&L_{\upsilon}\tau=L^e:d-L^{th}\dot{\vartheta}-\\&-[(L^e+\boldsymbol{g}\tau+\tau\boldsymbol{g}+W):\mathbf{P}]\frac{1}{T_m}\langle\Phi(\frac{f}{\kappa}-1)\rangle\end{aligned} \quad (53)$$

where

$$\begin{aligned}&L^e=\rho_{Ref}\,\frac{\partial^2\hat{\psi}}{\partial\mathbf{e}^2},\quad L^{th}=-\rho_{Ref}\,\frac{\partial^2\hat{\psi}}{\partial\mathbf{e}\partial\vartheta}\\&W=\eta^*[(\mathbf{g}\tau-\tau\mathbf{g}):(\alpha\mathbf{g}-\mathbf{g}\alpha)]\end{aligned} \quad (54)$$

Substituting $\dot{\psi}$ into the energy balance equation and taking into account the results $(51)_3$ and (52) gives

$$\rho\vartheta\dot{\eta}=-\mathrm{div}\mathbf{q}+\rho\vartheta\hat{i}. \quad (55)$$

Operating on the entropy relation $(51)_2$ with the Lie derivative and substituting the result into (55) we obtain

$$\rho c_p\dot{\vartheta}=-\mathrm{div}\mathbf{q}+\frac{\rho}{\rho_{Ref}}\frac{\partial\tau}{\partial\vartheta}:\mathbf{d}+\rho\chi^*\tau:\mathbf{d}^p+\rho\chi^{**}\mathbf{K}:L_{\upsilon}\xi \quad (56)$$

where the specific heat

$$c_p=-\vartheta\,\frac{\partial^2\hat{\psi}}{\partial\vartheta^2},\quad \chi^{**}\mathbf{K}=-\left(\frac{\partial\hat{\psi}}{\partial\vartheta}-\vartheta\,\frac{\partial^2\hat{\psi}}{\partial\vartheta\partial\xi}\right) \quad (57)$$

and χ^* and χ^{**} are the irreversibility coefficients.

6.8. Fracture criterion based on the evolution of microdamage

We base the fracture criterion on the evolution of the microdamage tensor ξ.

Let us assume that for $(\xi:\xi)^{\frac{1}{2}}=\xi^F$ catastrophe takes place (cf. Perzyna 1984), that is

$$\kappa=\hat{\kappa}(\varepsilon^p,\vartheta,\xi)\Big|_{(\xi:\xi)^{\frac{1}{2}}=\xi^F}=0. \quad (58)$$

It means that for $(\xi:\xi)^{\frac{1}{2}}=\xi^F$ the material loses its carrying capacity. The condition (58) describes the main feature observed experimentally that the load tends to zero at the fracture point.

In is noteworthy that the isotropic hardening-softening material function $\hat{\kappa}$ proposed in Eq. $(34)_1$ i should satisfy the fracture criterion (58).

7. ANALYSIS OF THE FUNDAMENTAL FEATURES OF THE MODEL

7.1. Invariance with respect to diffeomorphism

Our description of the thermo-elasto-viscoplastic constitutive structure is invariant with respect to any diffeomorphism. It means that the constitutive structure is invariant to any superposed motion. Such constitutive structure is called covariant, (cf. Marsden and Hughes 1983).

The covariance property of the constitutive structure has been achieved due to the assumption that the rates of the deformation tensors and the stress tensors (as well as all vectors and tensors) are defined based on the Lie derivative. Of course, the covariance description has very important consequence for proper mathematical investigations of some phenomena which can be discussed in the solution of the evolution problems. It will be also very crucial for proper description of meso-, micro-, and nano-mechanical problems and particularly in their numerical solutions.

7.2. Finite plastic deformation and plastic spin effects

The kinematics of finite elasto-viscoplastic deformation is based on notions of the Riemann space on manifolds and tangent spaces, (cf. Marsden and Hughes 1983). A multiplicative decomposition of the deformation gradient into elastic and viscoplastic parts is assumed. The viscoplastic spin has been also taken into account in the constitutive structure.

Due to these assumptions we obtain the consistent description of finite elasto-viscoplastic deformations. The main effect generated by the viscoplastic spin can be observed from the rate type constitutive relation for the Kirchhoff stress tensor τ (cf. Eq. (53)). In this equation the additional term $\frac{1}{T_m}\langle\Phi(\frac{f}{\kappa}-1)\rangle W:\boldsymbol{P}$ describes the influence of the viscoplastic spin.

7.3. Plastic non-normality

Plastic non-normality (i.e. $\mathbf{P} \neq \mathbf{Q}$ is generated by the influence of microdamage mechanisms. This effect is clear from the comparison of **P** (cf. Eq. (35)) and **Q** (cf. Eq. (50)). It has very important influence on the description of localization and localized fracture phenomena.

7.4 . Softening effects generated by microdamage mechanisms

By introducing the internal state variable ξ, i.e. the microdamage tensor in the constitutive structure the description of the intrinsic microdamage process has been achieved. From the available experimental observations we learn that there are three main mechanisms responsible for the evolution of microdamage, namely nucleation, growth and coalescence of microcracks. Taking advantage of the conjecture that coalescence mechanism can be treated as nucleation and growth process on a small scale we simplified the description of the intrinsic microdamage by making allowance only for the nucleation and growth mechanisms.

From the fundamental rate equation for temperature ϑ (cf. Eq. (56)) we observe that the micro-damage mechanism generates dissipation effects. On the other hand from the form of the isotropic work-hardening-softening function κ (cf. Eq. (34)) we see the direct description of softening effects caused by the intrinsic microdamage process.

It is noteworthy to add that the fundamental fracture criterion (cf. Eq. (58)) is also based on the evolution of microdamage.

7.5. Anisotropic effects in microdamage mechanisms

The induced anisotropy generated by the microdamage machanisms is described by the internal state variable ξ, i.e. the microdamage tensor.

Kinetic equation for ξ takes into account the influence of the stress triaxiality and anisotropic effects on the nucleation and growth mechanisms.

7.6. Plastic deformation induced anisotropic effects

Experimental observations of plastic flow processes have shown that finite plastic deformations induced the effect of anisotropy of a material. To describe this effect the residual stress (the back stress) α has been introduced to the constitutive structure as the internal state variable. The aim of this is to take into account the kinematic hardening phenomenon, which can be treated as first approximation of the description of plastic deformation induced anisotropy.

The evolution equation postulated for the back stress α represents the linear combination of the Prager and Ziegler kinematic hardening rules and additionally depends on the microdamage tensor ξ.

This kind of anisotropy generated by the kinematic hardening law will have very important influence on the localized fracture phenomena in thermo-viscoplastic flow processes under cyclic dynamic loadings.

7.7. Thermomechanical couplings (thermal plastic softening and thermal expansion)

An analysis of thermomechanical coupling effects can be based on the investigation of the evolution problem formulated for a thermo-elasto-viscoplastic model. Thermal expansion effect influences the fundamental, adiabatic, elastodynamic matrix *IE* for an adiabatic process, so it can have very important influence on the propagation and interaction of the deformation waves.

On the other hand the thermal plastic softening as typical dissipative effect influences an adiabatic process through the nonlinear function **f**. Of course, it will have a lot of influence on the localization phenomena as well as on the fracture phenomena.[6)]

7.8. Influence of stress triaxiality on the evolution of microdamage

The introduced modification of the kinetics of microdamage leads to the description of the influence of stress triaxiality. This has been done by assumption that the stress intensity invariants for nucleation and growth depend on the three invariants of stress tensor, cf. Eqs (43) and (44).

It has been shown by Dornowski and Perzyna (1999, 2000, 2002) that this modification helps to describe the accumulation of damage during dynamic loading process.

7.9. Rate sensitivity

To analyse the influence of the strain rate effect let as write the evolution constitutive equation (32) i in the form as follows

$$\left\|\mathbf{d}^P\right\| = \frac{1}{T_m}\langle\Phi(\frac{f}{\kappa}-1)\rangle\left\|\mathbf{P}\right\| \tag{59}$$

where $\|\cdot\|$ denotes the norm of the vectors in the 6-dimensional space. The equation (59) yields the following dynamical yield criterion

$$f = \hat{\kappa}(\varepsilon^P, \vartheta, \xi)\left\{1+\Phi^{-1}\left[T_m^0\phi_1(f_{ms})\phi_2(\dot{\varepsilon}^P)\frac{\left\|\mathbf{d}^P\right\|}{\left\|\mathbf{P}\right\|}\right]\right\} \tag{60}$$

[6)] For a thorough analytical discussion of the thermal plastic softening and thermal expansion effects on the localization of plastic deformation please consult the papers by Duszek-Perzyna and Perzyna (1994, 1998).

This relation may be interpreted as a description of actual change of the yield surface during the ther-modynamical process. This change is caused by isotropic and anisotropic work-hardening-softening effects, by the evolution of substructure and dependence on temperature and by the influence of the strain rate effects. It is noteworthy to add that the relation (60) constitutes a basis for experimental investigations which seek to examine the theoretical assumptions, (cf. Fig. 21).

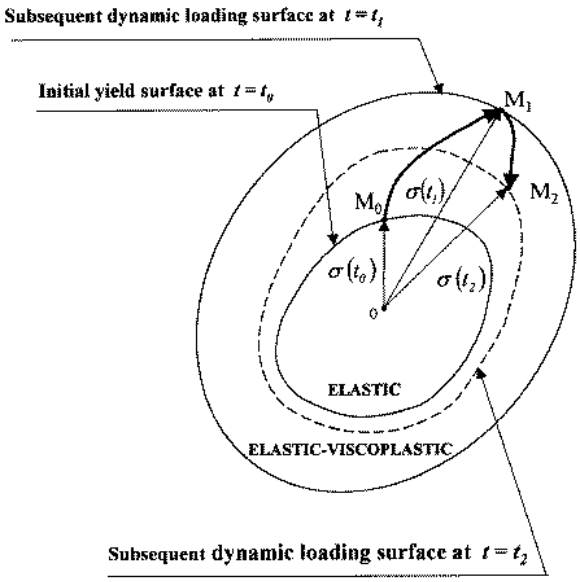

Fig. 21. Dynamic loading surface for the elasto-viscoplastic response

7.10. Length-scale sensitivity of the constitutive model

The constitutive equations for a thermo-elastic-viscoplastic model introduce implicitly a length-scale parameter into the dynamic initial-boundary value problem, i.e.

$$l = \beta c T_m \quad \text{or} \quad l = \beta c T_m^0 \phi_1(f_{ms}) \phi_2(\dot{\varepsilon}^P) \tag{61}$$

and as example for mild steel we have

$$l = \beta c T_m^0 \left[1 - f_{ms}^0 \frac{1}{1+\exp(a - b\varepsilon^P)}\right]\left(\frac{\dot{\varepsilon}^P}{\dot{\varepsilon}_s^P} - 1\right)^{\frac{1}{7}} \tag{62}$$

here T_m is the relaxation time for mechanical disturbances, and is directly related to the viscosity of the material, c denotes the velocity of the propagation of the elastic waves in the problem under consideration, and the proportionality factor β depends on the particular initial-boundary value problem and may also be conditioned on the microscopic properties of the material.

The relaxation time T_m can be viewed either as a microstructural parameter to be determined from experimental observations or as a mathematical regularization parameter.

It is noteworthy to stress that the length-scale sensitivity of the constitutive structure is of great importance for proper description of mesomechanical problems.

7.11. Dissipation effects

We observe that for an adiabatic process **dissipation effects** are generated by following phenomena:

(i) viscoplastic flow;
(ii) viscoplastic deformation induced anisotropy;
(iii) microdamage mechanisms.

For an adiabatic process ($\mathbf{q} = 0$) Eq. (56) takes the form

$$c_p \dot{\vartheta} = \vartheta \frac{1}{\rho_{Ref}} \frac{\partial \tau}{\partial \vartheta} : \mathbf{d} + \chi^* \tau : \mathbf{d}^P + \chi^{**} \mathbf{K} : L_\upsilon \xi \tag{63}$$

When the nondissipative term is neglected, then Eq. (63) takes the form

$$c_p \dot{\vartheta} = \chi^* \tau : \mathbf{d}^P + \chi^{**} \mathbf{K} : L_\upsilon \xi \tag{64}$$

From Eq. (64) we can compute the irreversibility coefficient χ^*. It gives

$$\chi^* = \frac{c_p \dot{\vartheta} - \chi^{**} \mathbf{K} : L_\upsilon \xi}{\tau : \mathbf{d}^P} \tag{65}$$

For $\chi^{**} = 0$, i.e. when the influence of the intrinsic microdamage mechanism is not taken into consideration, Eq. (65) takes the form

$$\chi^* = \frac{c_p \dot{\vartheta}}{\tau : \mathbf{d}^P} \tag{66}$$

For this particular case the irreversibility coefficient χ^* has a simple interpretation as the heat rate conversion to plastic work rate fraction. However, Eq. (65) shows that the remaining work rate is attributed to the energy rate lost for microdamage effects.

When modelling thermomechanical behaviour of materials, χ^* is usually assumed to be a constant in the range 0.85–0.95 (a practice that dates back to the work of Taylor and Quinney (1934)).

Recent experimental investigations performed by Mason *et al*. (1994) by using a Kolsky (split Hopkinson) pressure bar and a high-speed infrared detector array have clearly shown that this assumption may not be correct for all metals, (cf. Fig. 22).

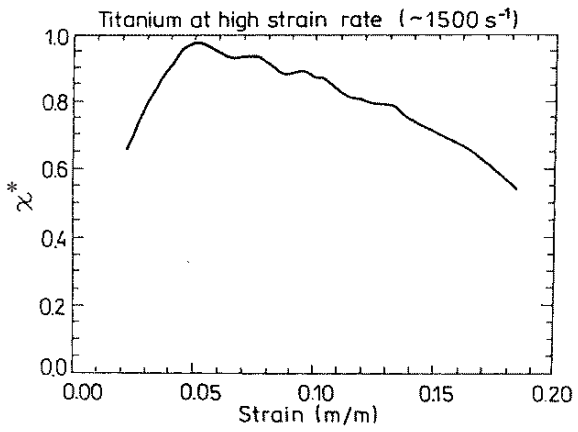

Fig. 22. The irreversibility coefficient χ^* versus strain calculated for Ti–6Al–4V titanium using the avarage of the temperature of the two detectors (after Mason *et al*. 1994)

The reason for this considerable discrepancy is clearly visible from Eq. (65). The rate of the stored energy implied by the evolution of microdamage is responsible for the decreasing of χ^* (e.g. as it has been observed for Ti–6Al–4V deformed at high strain rates).

7.12. Dispersion effects

It is very well known fact that the stress wave propagation in an elasto-viscoplastic medium has the dispersive nature.

The dispersion effect is very crucial for the development of the regularization procedure for the rate independent plastic flow evolution problems, cf. Section 7.14.

Of course, the dispersion effects will also influence very much the initiation and development of localization phenomena. A thorough analysis of these consequences has been presented in Glema, Lodygowski and Perzyna (2000, 2001, 2003).

7.13. Regularization of the evolution problem

Very recently, it has been widely recognized to consider an elastic-viscoplastic model of a material as a regularization method for solving mesh-dependent problems of plasticity. In these regularized initial-boundary value problems, wave propagation phenomena play a fundamental role. An elastic--viscoplastic model introduces dissipative as well as dispersive nature for the propagated waves. The dispersion property implies that in the elastic-viscoplastic medium any initial disturbance can break up into a system of group of oscillations or wavelets. On the other hand, the dissipation property causes the amplitude of a harmonic wavetrain to decay with time. In the evolution problem considered in such dissipative and dispersive medium, the stress deformation due to wave reflections and interactions are not uniformly distributed, and this kind of heterogeneity can lead to strain localization in the absence of geometrical or material imperfections.

7.14. Synergetic effects generated by cooperative phenomena

The question arises as follows: can cooperative phenomena described by a thermo-elasto-viscoplastic model lead to some synergetic effects.

This fundamental question has not easy answer. However, some investigations of the influence of synergetic effects on localization phenomena have been already presented, cf. for single crystals: Duszek-Perzyna and Perzyna (1993, 1996), Duszek-Perzyna, Korbel and Perzyna (1997), Perzyna and Korbel (1996, 1998) and Perzyna (1998, 2002); and for polycrys-talline solids: Duszek-Perzyna and Perzyna (1991, 1994, 1995, 1998) and Perzyna (1994, 1995, 1998). Numerical investigation of synergetic effects for localization and fracture phenomena has been given in Duszek-Perzyna and Perzyna (1994, 1998) and Lodygowski and Perzyna (1997).

8. EPILOGUE

The experimental works have brought deep understanding of the evolution of the dislocation substructure and the intrinsic microdamage mechanism during dynamic loading processes and clearly have shown that microshear banding influence a substructure of a polycrystalline material and fracture mechanism of metals does very much depend on the strain rate and wave shape effects.

The crucial idea in this theory is the very efficient interpretation of a finite set of the internal state variables as the equivalent plastic deformation, the microdamage tensor and the residual stress (the back stress). To describe suitably the time and temperature dependent effects observed experimentally and the accumulation of the plastic deformation and anisotropic damage during dynamic loading processes the thermomechanical coupling has been taken into account and the kinetics of microdamage and kinematic hardening law have been modified and generalized.

Since the rate independent plastic response is obtained as the limit case when the relaxation time is equal to zero hence the theory of elasto-viscoplasticity offers the regularization procedure for the solution of the dynamical initial-boundary value problems. The viscoplastic regularization procedure assures the stable integration algorithm by using the finite difference or finite element methods.

There is our hope that this thermodynamical theory of elasto-viscoplasticity may be used as a basis for the description of the behaviour of modern materials, particularly nanometals (cf. Meyers, Mishra and Benson (2006), Jia, Ramesh and Ma (2003) and Korbel, Nowak, Perzyna and Pe·cherski (2006)) and the investagation of plastic strain localization and localized fracture phenomena in meso-, micro-, and nano-mechanical processes.

Acknowledgement

This work has been prepared within:

(i) the Polish–USA Joint Research Project for years 2004–2006, under the Agreement of Scientific Cooperation between The Polish Academy of Sciences and the National Science Foundation (USA): "Localization and Fracture under Dynamic Loading Processes in Mesomechanics Problems";

(ii) the framework of the Research Project PBZ-KBN-096/T08/2003.

REFERENCES

Abraham R., Marsden J.E. 1988: *Foundations of Mechanics*. Second Edition, Addison–Wesley, Reading Mass., 1978.

Abraham R., Marsden J.E., Ratiu T. 1988, *Manifolds, Tensor Analysis and Applications*. Springer, Berlin 1988.

Barbee T.W., Seaman L., Crewdson R., Curran D. 1972: *Dynamic fracture criteria for ductile and brittle metals*. J. Mater., 7, 393–401.

Bassani J.L. 1994: Plastic flow of crystals. Adv. Appl. Mech., 30, 191–258.

Boehler J.P. (Ed.) 1990: *Yielding, Damage, and Failure of Anisotropic Solids*. Proc. IU-TAM/ICM Symposium, Villard-de Lans, 24–28 August 1987, Mech. Eng. Public. Limited, London 1990.

Campbell J.D., Ferguson W.G. 1970: T*he temperature and strain-rate dependence of the shear strength of mild steel*. Phil. Mag., 81, 63–82.

Chang Y.W., Asaro R.J. 1980: *Lattice rotations and shearing in crystals*. Arch. Mech., 32, 369–388.

Coleman B.D., Noll W. 1963: *The thermodynamics of elastic materials with heat conduction and viscosity*. Arch. Rational Mech. Anal., 13, 167–178.

Curran D.R., Seaman L., Shockey D.A. 1977: *Dynamic failure in solids*. Physics Today, January, 46–55.

Curran D.R., Seaman L., Shockey D.A. 1981: *Linking dynamic fracture to microstructural processes*. [in:] Shock Waves and High-Strain Rate Phenomena in Metals: Concepts and Curran, D.R., Seaman, L., Shockey, D.A. 1987, Dynamic failure of solids, Physics Reports, 147, 253–388.

Dafalias Y.F. 1983: *Corotational rates for kinematic hardening at large plastic deformations*. J. Appl. Mech., 50, 561–565.

Dornowski W., Perzyna P. 1999: *Constitutive modelling of inelastic solids for plastic flow processes under cyclic dynamic loadings*. Transaction of the ASME, J. Eng. Materials and Technology, 121, 210–220.

Dornowski W., Perzyna P. 2000: *Localization phenomena in thermo--viscoplastic flow processes under cyclic dynamic loadings*. Computer Assisted Mechanics and Engineering Sciences, 7, 117–160.

Dornowski W., Perzyna P. 2002: *Numerical analysis of macrocrack propagation along a bima-terial interface under dynamic loading processes*. Int. J. Solids and Structures 39, 4949–4977.

Dowling A.R., Harding J., Campbell D.J. 1970: *The dynamic punching of metals*. J. Inst. of Metals, 98, 215–224, 1970.

Duszek M.K., Perzyna P. 1991a: *On combined isotropic and kinematic hardening effects in plastic flow processes*. Int. J. Plasticity, 7, 351–363.

Duszek M.K., Perzyna P. 1991b: *The localization of plastic deformation in thermoplastic solids*. Int. J. Solids Structures, 27, 1419–1443.

Duszek-Perzyna M.K., Korbel K., Perzyna P. 1997: *Adiabatic shear band localization in single crystals under dynamic loading processes*. Arch. Mechanics, 49, 1069–1090.

Duszek-Perzyna M.K., Perzyna P. 1993: *Adiabatic shear band localization in elastic-plastic single crystals*. Int. J. Solids Structures, 30(1), 61–89.

Duszek-Perzyna M.K., Perzyna P. 1994: *Analysis of the influence of different effects on criteria for adiabatic shear band localization in inelastic solids*. [in:] Material Instabilities: Theory and Applications, ASME Congress, Chicago, 9–11 November 1994, Batra R.C., Zbib H.M. (Eds), AMD, vol. 183/MD, Vol. 50, ASME, New York, 1994, 59–85.

Duszek-Perzyna M.K., Perzyna P. 1995: A*cceleration waves in analysis of adiabatic shear band localization*. [in:] Nonlinear Waves in Solids, Proc. IUTAM Symposium, August 15–20, 1993, Victoria, Canada; Wegner J.L., Norwood F.R. (Eds), 128–135, ASME Book No AMR, 137, 1995.

Duszek-Perzyna M.K., Perzyna P. 1996: *Adiabatic shear band localization of inelastic single crystals in symmetric double slip process*. Archive of Applied Mechanics, 66, 369–384.

Duszek-Perzyna M.K., Perzyna P. 1998: *Analysis of anisotropy and plastic spin effects on localization phenomena*. Arch. Appl. Mechanics, 68, 352–374.

Follansbee P.S. 1986: *Metallurgical Applications of Shock – Wave and High-Strain-Rate Phenomena*. Murr L.E., Staudhammer K.P., Meyeres M.A. (eds), 451–480, Marcel Dekker, New York, 1986.

Glema A., Lodygowski T., Nowak Z., Perzyna P., Voyiadjis G.Z. 2005: *Thermo-elasto-visco-plastic model of a material with non-local and anisotropic intinsic microdamage*. McMat 2005, Mechanics and Materials Conference, June 1–3, 2005, Baton Rouge, LA, USA.

Glema A., Lodygowski T., Perzyna P. 2000: *Interacton of deformation waves and localization phenomena in inelastic solids*. Computer Methods in Applied Mechanics and Engineering, 183, 123–140.

Glema A., Lodygowski T., Perzyna P. 2001: *The role of dispersion for the description of strain localization in materials under impact loading*. European Conference on Computational Mechanics, June 26–29, Cracow, Poland, 2001.

Glema A., Lodygowski T., Perzyna P. 2003: *Localization of plastic deformations as a result of wave interaction*. CAM&ES, 3, 81–91.

Glema A., Lodygowski T., Perzyna P., Sumelka W. 2006: *Constitutive anizotropy induced by plastic strain localization*. 35th Solid Mechanics Conference, Krakow, Poland, September 4–8, 2006.

Grebe H.A., Pak H.R., Meyers M.A. 1985: *Adiabatic shear band localization in titanium and Ti-6PctAl-4PctV alloy*. Met. Trans., 16A, 761-775.

Jia D., Ramesh K., Ma E. 2003: *Effects on nanocrystalline and ultrafine grain sizes on constitutive behaviour and shear bands in iron*. Acta Materialia, 51, 3495–3509.

Johnson J.N. 1981: *Dynamic fracture and spallation in ductile solids.* J. *Appl. Phys., 52, 2812–2825.*

Korbel K., Nowak Z., Perzyna P., Pecherski R.B. 2006: *Viscoplasticity of nanometals based on Burzyński yield condition*. 35th Solid Mechanics Conference, Krakow, Poland, September 4–8, 2006.

Kumar A., Kumble R.Gg. 1969: *Viscous drag on dislocations at high strain rates in copper*. J. Appl. Physics, 40, 3475–3480.

Lisiecki L.L., Nelson D.R., Asaro R.J. 1982: *Lattice rotations, necking and localized deformation in f.c.c. single crystals*. Scripta Met., 16, 441–449.

Loret B. 1983: *On the effects of plastic rotation in the finite deformation of anisotropic elasto-plastic materials*. Mech. Mater., 2, 287–304.

Lodygowski T., Perzyna P. 1997: *Numerical modelling of localized fracture of inelastic solids in dynamic loading processes*. Int. J. Num. Meth. Engng., 40, 4137–4158.

Lodygowski T. Perzyna P. 1997: *Localized fracture of inelastic polycrystalline solids under dynamic loading processes*. Int. J. Damage Mechanics, 6, 364–407.

Marsden J.E., Hughes T.J.R. 1983: *Mathematical Foundations of Elasticity*. Prentice-Hall, Englewood Cliffs, New York 1983.

Mason J.J., Rosakis J.A., Ravichandran R. 1994: *On the strain and strain rate dependence of the fraction of plastic work converted to heat: an experimental study using high speed infrared detectors and the Kolsky bar*. Mechanics of Materials, 17, 135–145.

Meyers H.C. 1994: *Dynamic Behaviour of Materials*. John Wiley, New York 1994.

Meyers M.A., Aimone C.T. 1983: *Dynamic fracture (spalling) of metals*. Prog. Mater. Sci., 28, 1–96.

Meyers M.A., Mishra A., Benson D.J. 2006: *Mechanical properties of nanocrystalline materials*. Prog. Mater. Sci., 51, 427–556.

Nemes J.A., Eftis J. 1993: *Constitutive modelling of the dynamic fracture of smooth tensile bars*. Int. J. Plasticity, 9, 243–270.

Nowak Z., Perzyna P., Pęcherski R.B., 2007: *Desription of viscoplastic flow accounting for shear banding*. Arch. Metallurgy and Materials, 52, 217–222.

Oldroyd J. 1950: *On the formulation of rheological equations of state*. Proc. R. Soc. Lond. A200, 523–541.

Perzyna P. 1963: *The constitutive equations for rate sensitive plastic materials*. Quart. Appl. Math., 20, 321–332.

Perzyna P. 1966: *Fundamental problems in viscoplasticity*. Advances in Applied Mechanics, 9, 343–377.

Perzyna P. 1971: *Thermodynamic theory of viscoplasticity*. Advances in Applied Mechanics, 11, 313–354.

Perzyna P. 1977: *Coupling of dissipative mechanisms of viscoplastic flow*. Arch. Mechanics, 29, 607–624.

Perzyna P. 1980: *Modified theory of viscoplasticity. Application to advanced flow and instability phenomena*. Arch. Mechanics, 32, 403–420.

Perzyna P. 1984: *Constitutive modelling of dissipative solids for postcritical behaviour and fracture*. ASME J. Eng. Materials and Technology, 106, 410–419.

Perzyna P. 1986a: *Internal state variable description of dynamic fracture of ductile solids*. Int. J. Solids Structures, 22, 797–818.

Perzyna P. 1986b: *Constitutive modelling for brittle dynamic fracture in dissipative solids*. Arch. Mechanics, 38, 725–738.

Perzyna P. 1988: *Temperature and rate dependent theory of plasticity of crystalline solids*. Revue Phys. Appl. 23, 445–459.

Perzyna P. 1994: *Instability phenomena and adiabatic shear band localization in thermoplastic flow processes*. Acta Mechanica, 106, 173–205.

Perzyna P. 1995: *Interactions of elastic-viscoplastic waves and localization phenomena in solids*. IUTAM Symposium on Nonlinear Waves in Solids, August 15–20, 1993, Victoria, Canada; Wegner J.L., Norwood F.R. (Eds), ASME 1995, 114–121.

Perzyna P. 1998: *Constitutive modelling of dissipative solids for localization and fracture*. [In:] Localization and Fracture Phenomena in Inelastic Solids, Perzyna P. (Ed.), Springer, Wien, New York, 1998, 99–242.

Perzyna P. 2001: *Thermo-elasto-viscoplasticity and damage*. In: Handbook of Materials Behaviour ModelsLemaitre J. (Ed.), Academic Press, New York, 821–834, 2001.

Perzyna P. 2002: *Thermodynamical theory of inelastic single crystals*. Engineering Transactions, 50, 107–164.

Perzyna P. 2005: *The thermodynamical theory of elasto-viscoplasticity*. Engineering Transactions, 53, 235–316.

Perzyna P., Drabik A. 1989: *Description of micro-damage process by porosity parameter for nonlinear viscoplasticity*. Arch. Mechanics, 41, 895–908.

Perzyna P., Drabik A. 2006: *Micro-damage mechanism in adiabatic processes*. Engineering Transactions (in print).

Perzyna P., Korbel K. 1996: *Analysis of the influence of substructure of crystal on the localization phenomena of plastic deformation*. Mechanics of Materials, 24, 141–158.

Perzyna P., Korbel K. 1998: *Analysis of the influence of variuos effects on criteria for adiabatic shear band localization in single crystals*. Acta Mechanica, 129, 31–62.

Perzyna P., Voyiadjis G.Z. 2005: *Thermodynamic theory of elasto-viscoplasticity for induced anisotropy effects*. McMat 2005, Mechanics and Materials Conference, June 1–3, 2005, Baton Rouge, LA, USA.

Pęcherski R.B. 1998: *Macroscopic effects micro-shear banding in plasticity of metals*. Acta Mechanica, 131, 203–224.

Rashid M.M., Gray G.T., Nemat–Nasser S. 1992: *Heterogeneous deformations in copper single crystals at high and low strain rates*. Philosophical Magazine, A, 65, 707–735, 1992.

Rosenfield A.R., Hahn G.T. 1966: *Numerical decsription of the ambient low-temperature, and high-strain rate flow and fracture behaviour of plain carbon steel*. Trans. Am. Soc. Metals, 59, 962–980.

Seaman L., Curran D.R., Shockey D.A. 1976: J. Appl. Phys., 47, 4814–4820.

Shima S., Oyane M. 1976: *Plasticity for porous solids*. Int. J. Mech. Sci., 18, 285–291.

Shockey D.A., Seaman L., Curran D.R. 1973: In: *Metallurgical Effects at High Strain Rates*. Rohde R.W., Butcher B.M., Holland J.R., Karnes C.H. (Eds), Plenum Press, New York 1973, 473.

Shockey D.A., Seaman L., Curran D.R. 1985: *The microstatistical fracture mechanics approach to dynamic fracture problem*. Int. J. Fracture, 27, 145–157.

Sidey D., Coffin L.F. 1979: *Low-cycle fatigue damage mechamisms at high temperature*. in: Fatigue Mechanisms, Proc. ASTM STP 675 Symposium, Kansas City, Mo., May 1978, Fong J.T. (Ed.), Baltimore, 1979, 528–568.

Spitzig W.A. 1981: *Deformation behaviour of nitrogenated Fe–Ti–Mn and Fe–Ti single crystals*. Acta Metall. 29, 1359–1377.

Taylor G.I., Quinney H. 1934: *The latent energy remaining in a metal after cold working*. Proc. R. Soc. Lond., A143, 307–326.

Teodosiu C., Sidoroff F. 1976: *A theory of finite elastoplasticity of single crystals*. Int. J. Engng. Sci., 14, 165–176.

Truesdell C., Noll W. 1985: *The Non-Linear Field Theories of Mechanics*. [in:] Handbuch der Physik III/3, Flugge S. (Ed.), Springer-Verlag, Berlin 1965.

Van der Giessen E. 1991: *Micromechanical and thermodynamic aspects of the plastic spin*. Int. J. Plasticity, 7, 365–386.

Voyiadjis G.Z., Ju J.–W., Chaboche J.–L. (Eds) 1998: *Damage Mechanics in Engineering Materials*. Elsevier, Amsterdam 1998.